Models for adatom diffusion on fcc (001) metal surfaces

Hanoch Mehl, Ofer Biham, and Itay Furman
Racah Institute of Physics, The Hebrew University, Jerusalem 91904, Israel

Majid Karimi
Physics Department, Indiana University of Pennsylvania, Indiana, Pennsylvania 15705
(Received 28 December 1998)

We present a class of models that describe self-diffusion on fcc (001) metal substrates within a common framework. The models are tested for Cu(001), Ag(001), Au(001), Ni(001), and Pd(001), and found to apply well for all of them. For each of these metals the models can be used to estimate the activation energy of any diffusion process using a few basic parameters that may be obtained from experiments, *ab initio* or semiempirical calculations. To demonstrate the approach, the parameters of the models are optimized to describe self-diffusion on the (001) surface, by comparing the energy barriers to a full set of barriers obtained from semiempirical potentials via the embedded atom method (EAM). It is found that these models with at most four parameters, provide a good description of the full landscape of hopping energy barriers on fcc (001) surfaces. The main features of the diffusion processes revealed by EAM calculations are quantitatively reproducible by the models. [S0163-1829(99)01227-8]

I. INTRODUCTION

Thin-film growth processes involve complicated kinetics giving rise to a rich variety of surface morphologies. Within this vast domain, the study of the growth in the submonolayer regime is of particular interest due to the large impact of the initial kinetics on the resulting film structure. Experiments on thin film growth on well-characterized substrates using molecular-beam epitaxy have provided a large body of information about growth kinetics and morphology, and revealed that for a variety of systems and a broad temperature range, island nucleation is the dominant mechanism for crystal growth.[1,2] Diffraction methods such as helium beam scattering,[1,3–6] low-energy electron diffraction,[7–10] and other techniques,[11,12] provide information on the collective behavior and the statistical properties of the surface. These techniques have been used to measure the island size distribution, the island density, and their scaling properties with respect to the coverage and the flux.[3,7–10] The variation of the island density with respect to the temperature was also studied.[3,9,11]

More detailed information at the atomic scale is provided by scanning tunneling microscopy (STM).[2,12–31] Most notably, STM provides means to study the variety of morphologies encountered in the different systems, or in the same system under different growth conditions.[2,12–20,23] In some experiments, STM was used to acquire information on larger scales, e.g., island size distributions.[12,14,20–22,26] Despite the wealth of experimental results at the atomic scale, for decay rates of small islands, mobility of small islands and edge diffusion,[21,23–27,29,31] the underlying energetics is mostly inaccessible to direct experimental measurements. Thus, one must rely on theory to extract activation energies from the experimental results, and these are usually limited in number, and sometimes are subject to alternative interpretations.

The only technique that provides direct access to diffusion processes and activation energies at the atomic scale is field ion microscopy.[32–36] This technique was used to identify the diffusion modes of adatoms[32,33] as well as small islands[34,36] on fcc (001) metal surfaces, to measure their diffusion coefficients, and to determine the sticking process of adatoms to an island.[35] Recently there were several attempts to use STM to derive such local information directly.[24]

Theoretical studies aimed at providing better understanding of the relation between key processes at the atomic scale and the resulting morphologies have been done using Monte Carlo simulations.[37–57] In simulations of island growth during deposition, atoms are deposited randomly on the substrate at rate F [given in monolayers per second] and then hop, attach to, and detach from existing islands according to some model. A common approach is to assume some key processes and their rates, and then simulate the growth process.[37,38,40,44] In some cases information such as diffusion length, typical distance and time between nucleation events is assumed to be known *a priori*, and is put by hand into the simulation in order to accelerate the computation.[46,48,58] The advantage of this approach is that the models are well defined and use only few parameters. These models are useful for studies of scaling and morphology but cannot provide a quantitative description of diffusion on a particular substrate. Furthermore, they account only for a limited number of processes, that are assumed to be the only significant ones.

A complementary scheme employs the underlying activation energies. In this scheme the hopping rate h (in units of hops per second) of a given atom to each unoccupied nearest-neighbor (NN) site is given by

$$h = \nu \exp(-E_B/k_B T), \tag{1}$$

where $\nu = 10^{12}\,\text{s}^{-1}$ is the commonly used attempt rate, E_B is the activation energy barrier, k_B is the Boltzmann constant, and T is the temperature.

The activation energy barrier E_B depends on the local environment of the hopping atom, namely the configuration

PRB <u>60</u>   2106

of occupied and unoccupied adjacent sites. Two approaches have been taken in the construction of the energy barriers for hopping in the simulations. One approach was to construct simple models that include the desired features, such as stability and mobility of small islands, and that take into account properties such as bond energies.[41,45,47,49–52,54,56] In general, this approach encompasses both the virtues and the drawbacks of the simpler approach presented before.

A second approach is based on the use of an approximate many-body energy functional to calculate the hopping energy barriers for a complete set of relevant configurations.[39,42,43,53,55,57] This approach provides a good description of diffusion processes on the given substrate but only limited understanding due to the large number of parameters.

In this paper, we extend and further explore a framework for a *systematic* derivation of simple models for self-diffusion on fcc (001) surfaces out of a detailed and complicated set of energy barriers. Simple in this context means that only a small number of parameters are involved and all have a definite and intuitive interpretation. Using sensible assumptions about the bond energies and diffusion paths we obtain simple formulas for the activation energy barriers. We then *optimize* the parameters of these formulas for each metal separately by using energy barriers obtained from the embedded-atom method. This procedure gives rise to simple models that have at most four parameters and provide good quantitative description of the landscape of hopping energy barriers. In a previous publication we have introduced the framework and applied it to Cu/Cu(001) growth.[59] Here, we make a threefold step forward. (a) We include four other fcc metals in the model and derive the appropriate parameters for them. This shows the utility of the models and provide a unifying framework that applies to a large class of metals; (b) Nonlinear interactions are introduced in addition to the linear interactions considered before. This allows for a more accurate optimization without increasing the number of parameters; (c) We explore the basis of the assumptions underlying this scheme and the extent of their applicability.

The paper is organized as follows. In Sec. II, we introduce the physical framework of the model and discuss its underlying assumptions. The results of the embedded-atom method (EAM) calculations are given in Sec. III. The models are introduced in Sec. IV with the fitting to the EAM results. This is followed by a discussion of the results and their implications in Sec. V.

II. APPLICABILITY CONSIDERATIONS

The framework developed in this paper assumes several characteristics of the diffusion processes considered. It applies to systems for which these assumptions are valid, which includes most of the fcc metals in the moderate temperature regime ($\approx$200–500 K). The following assumptions are employed throughout the discussion.

Bridge-site hopping of adatoms is in general dominant over exchange hopping (Fig. 1). There has been a controversy concerning this assumption. Using semiempirical methods the barrier for exchange hopping for Cu(001) was estimated to be 0.2 eV,[60–62] in agreement with the experimental data that was available at that time.[3] This is much

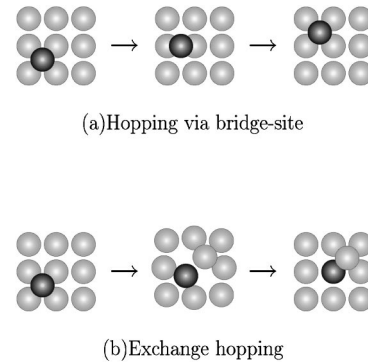(a)Hopping via bridge-site

(b)Exchange hopping

FIG. 1. Two mechanisms for surface diffusion: (a) regular or bridge-site hopping; (b) exchange hopping. Dark spheres are adatoms and light spheres are substrate atoms.

lower than the barrier for bridge-site hopping. However, theoretical work using several other methods,[63–65] including EAM, indicate that the exchange barrier for Cu is much higher (more than 0.8 eV) and therefore bridge-site hopping is dominant. This conclusion is also supported by recent experimental work and reinterpretation of the previous findings.[9] In general, bridge-site hopping is found to be dominant in all the metals studied here. (for Au, some exchange processes appear to be significant, yet in most cases bridge hopping is favorable). Due to the exponential dependence of the rate of each process on the corresponding energy barrier, it is generally reasonable to take into account only the mechanism that is energetically favorable (bridge-site hopping, in this case) and neglect the mechanism that exhibits higher activation energy barrier (exchange mechanism).

Only nearest and next-nearest neighbor interactions are significant. Within this assumption one can obtain the activation energies for most diffusion processes to a good accuracy. However, there are some processes such as vacancy diffusion, where a larger environment affects the diffusing atom.

There is one common attempt frequency for all processes. Since there is no systematic knowledge about the dependence of the attempt frequency on the local environment, the assumption of one common frequency is the usual practice. Estimations for the attempt frequency can be obtained using molecular-dynamic simulations.[64] Another way is to fit molecular static data to harmonic potential to find an effective force constant, and then deduce the frequency of oscillations. So far, little work has been done on this subject. Previous works, including interpretation of experimental results, usually pre-suppose some common attempt frequency in the range $10^{12}-10^{13}$ s^{-1}.[66]

III. THE EAM BARRIERS

The models described in this work are tested by fitting their parameters to energy barriers for self-diffusion of Cu(001), Ag(001), Au(001), Ni(001), and Pd(001) surfaces, obtained using EAM.[67] This method uses semiempirical potentials and provides a good description of self diffusion on such surfaces.[65] Specifically, for all the metals considered here the EAM functions developed by Adams, Foiles, and Wolfer[68] are employed. These functions are fitted to a similar but more accurate data base as the one employed by Foiles, Baskes, and Daw.[69] The calculations are done on a slab of 20
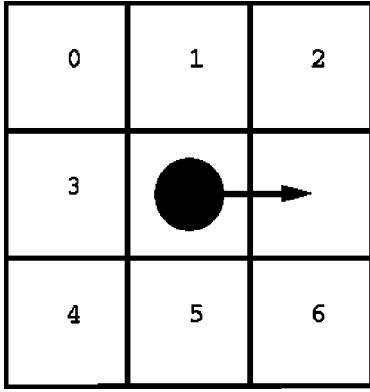
FIG. 2. Classification of all possible local environments of a hopping atom, including seven adjacent sites. Each site can be either occupied or unoccupied, giving rise to $2^7 = 128$ local environments. Sites 1, 3, and 5 are nearest neighbors of the original site while sites 1, 2, 5, and 6 are adjacent to the bridge site that the atom has to pass.

square layers with 100 atoms in each layer.

When an atom on the surface hops into a vacant nearest-neighbor site it has to cross the energy barrier between the initial and final sites. We have used molecular statics in conjunction with the EAM functions to find that energy barrier. This is simply the difference between the energy at the bridge site (or more precisely, at the point along the path with highest energy) and in the initial site.

The hopping energy barriers are calculated for all local environments as shown in Fig. 2, where seven adjacent sites, $i = 0, \ldots, 6$ are taken into account, according to the assumptions presented in Sec. II. Each one of these sites can be either occupied ($S_i = 1$) or vacant ($S_i = 0$), giving rise to $2^7 = 128$ barriers. A binary representation is used to assign indices to these barriers. For each configuration ($S_0, \ldots, S_6$) the barrier is given by E_B^n, where

$$n = \sum_{i=0}^{6} S_i 2^i \qquad (2)$$

takes the values $n = 0, \ldots, 127$. The full set of hopping energy barriers (given in eV) is presented in Table I, for Cu(001), Ag(001), Au(001), Ni(001), and Pd(001). To show these values in a compact form, each barrier in Table I corresponds to a configuration in which the occupied sites are the union of the occupied sites in the picture on top of the given column and on the left-hand side of the given row. The column in Table I in which a given configuration appears is determined by the occupancy of sites $i = 2, 3, 6$ while the row is determined by sites $i = 0, 1, 4, 5$. One can define

$$n_1 = \sum_{i=2,3,6} S_i 2^i; \quad n_2 = \sum_{i=0,1,4,5} S_i 2^i; \qquad (3)$$

such that for each configuration $n = n_1 + n_2$. To demonstrate the use of Table I, we will check for Cu(001) the barrier of the configuration in which sites 0, 3, and 4 are occupied and all other sites adjacent to the hopping atom are vacant. For this configuration, according to Eq. (3), $n_1 = 8$ and n_2

$= 17$ ($n = 25$). The barrier, that is found in the column with the index 8 and the row with index 17, in the line of Cu, is $E_B^{25} = 0.89$ eV.

In Table I, we use the symmetries of the configurations in the 3×3 cell (Fig. 2) to reduce the number of entries. There is a mirror symmetry plane perpendicular to the surface and containing the arrow of the hopping atom. Consequently, the columns of $n_1 = 4$ and 12, in which site $i = 2$ is occupied, stand also for the symmetric configurations in which $i = 6$ is occupied. In the other four columns, there are some configurations that, due to symmetry, appear twice. In such cases, the barrier for the configuration with larger n appears in *italics*.

For the purpose of the calculations and parameterization of the model, we consider only hopping moves in which a single atom hops each time. It turns out, however, that in some cases the molecular statics calculations, used to obtain the barriers, give rise to concerted moves. In such moves the atom at site $i = 3$ follows the hopping atom and takes the place vacated by the hopping atom. This fact significantly reduces the barrier. It turns out that for configurations in which concerted moves appear, they can be suppressed by adding a column of three atoms on the left-hand side of sites $i = 0, 3$, and 4. In Table I, the energy values for those configuration in which a concerted move was found, are shown in parenthesis. The barrier obtained when the concerted move was suppressed is shown to the left of the parenthesis.

To gain a better understanding of the barrier energy landscape we present the barrier height distribution (without concerted moves) in Fig. 3 for the five metals considered. We observe that this distribution exhibits four groups. This feature is in agreement with Ref. 43 where a different method[70] was used to calculate the barriers. Each group corresponds to a single or a double column in Table I. In general, group I includes very fast moves towards island edges, group II includes moves along the edge, group III includes, most notably, the single atom move, while group IV includes detachment moves.

IV. THE MODELS

A. The additivity assumption

The starting point in the construction of a simple model that describes the hopping energy barriers for all the configurations of Fig. 2, is the assumption that the contributions of all adjacent atoms to the energy barrier add up linearly. To examine this assumption for Cu(001), we evaluated directly the binding energies within the EAM approach for a series of configurations from which we extracted the relevant bond energies.

The binding energy of a given configuration of adatoms on the surface is evaluated as follows: First, we calculate the total energy of the system in that configuration. Then, we find the total energy of another configuration in which there is the same number of adatoms on the surface but they are far apart from each other (by that we mean that moving them one lattice site in any direction would not change the total energy). The binding energy between the adatoms is given by the difference in the total energies between the two configurations. An example of the procedure is shown in Fig. 4. It appears that the evaluation of the next nearest-neighbor

TABLE I. The hopping energy barriers for Cu, Ag, Au, Ni, and Pd obtained from the EAM calculations for all possible configurations within a 3×3 square around the hopping atom. The barriers are given in eV. Each number in the table is the barrier E_B^n for the configuration in which the occupied sites are the union of the occupied sites in he picture on top of the given column (indexed by n_1) and on the left-hand side of the given row (indexed by n_2). Consequently, the index n specifying the barrier is given by $n=n_1+n_2$.

$n_2\downarrow$ / $n_1\rightarrow$		Group I 68	Group 76	II 4	Group 12	III 0	Group IV 8
0		Cu 0.01	0.25	0.18	0.48	0.48	0.81
		Ag 0.16	0.37	0.23	0.47	0.48	0.72
		Au 0.37	0.64	0.45	0.72	0.70	1.02
		Ni 0.06	0.38	0.25	0.62	0.63	1.02
		Pd 0.15	0.48	0.34	0.70	0.71	1.08
1		Cu 0.02	0.28	0.25	0.53	0.46	0.85
		Ag 0.16	0.37	0.24	0.46	0.48	0.72
		Au 0.31	0.54	0.39	0.61	0.64	0.85
		Ni 0.09	0.40	0.30	0.66	0.69	1.05
		Pd 0.15	0.47	0.33	0.69	0.70	1.07
2		Cu 0.02	0.21	0.18	0.44 (0.34)	0.46	0.74 (0.60)
		Ag 0.15	0.35	0.22	0.45	0.48	0.72
		Au 0.30	0.56	0.38	0.62	0.79	1.00
		Ni 0.09	0.35 (0.10)	0.26	0.57 (0.48)	0.61	0.95 (0.79)
		Pd 0.16	0.43 (0.38)	0.33	0.68	0.74	1.10 (0.91)
3		Cu 0.05	0.25	0.24	0.48	0.54	0.78 (0.65)
		Ag 0.16	0.35	0.23	0.45	0.50	0.72
		Au 0.27	0.52	0.36	0.61	0.77	1.00
		Ni 0.13	0.35 (0.33)	0.31	0.63	0.68	0.99
		Pd 0.17	0.49	0.35	0.70	0.77	1.13
16		*Cu 0.02*	*0.28*	0.21	0.50	*0.46*	*0.85*
		Ag 0.16	*0.37*	0.24	0.47	*0.48*	*0.72*
		Au 0.31	*0.54*	0.38	0.67	*0.64*	*0.85*
		Ni 0.09	*0.40*	0.30	0.65	*0.69*	*1.05*
		Pd 0.15	*0.47*	0.33	0.69	*0.70*	*1.07*
17		Cu 0.04	0.30	0.28	0.54	0.66	0.89
		Ag 0.17	0.36	0.24	0.47	0.49	0.72
		Au 0.26	0.57	0.34	0.60	0.59	0.83
		Ni 0.13	0.43	0.35	0.68	0.75	1.09
		Pd 0.15	0.48	0.34	0.70	0.71	1.07
18		Cu 0.05	0.27	0.23	0.49	0.52	0.80
		Ag 0.16	0.35	0.22	0.44	0.49	0.72
		Au 0.26	0.57	0.34	0.55	0.75	0.98
		Ni 0.12	0.40	0.30	0.63	0.66	1.01
		Pd 0.17	0.48	0.34	0.68	0.75	1.11
19		Cu 0.08	0.29	0.29	0.52	0.61	0.83
		Ag 0.17	0.35	0.24	0.45	0.51	0.73
		Au 0.26	0.54	0.32	0.64	0.82	0.99
		Ni 0.16	0.42	0.36	0.66	0.74	1.04
		Pd 0.19	0.50	0.37	0.72	0.79	1.15
32		*Cu 0.02*	*0.21*	0.18	0.48	*0.46*	*0.74 (0.60)*
		Ag 0.15	*0.35*	0.31	0.54	*0.48*	*0.72*
		Au 0.30	*0.56*	0.61	0.86	*0.76*	*1.00*
		Ni 0.09	*0.35 (0.10)*	0.32	0.65 (0.52)	*0.61*	*0.95 (0.79)*
		Pd 0.16	*0.43 (0.38)*	0.46	0.77 (0.66)	*0.74*	*1.10*

TABLE I. (*Continued.*)

$n_2\downarrow$			Group I 68	Group 76	II 4	Group 12	III 0	Group IV 8
33		Cu	0.05	0.27	0.28	0.54	0.52	0.80
		Ag	0.16	0.35	0.32	0.54	0.49	0.72
		Au	0.26	0.57	0.58	0.81	0.74	0.98
		Ni	0.12	0.40	0.38	0.69 (0.64)	0.66	1.01
		Pd	0.17	0.48	0.47	0.83	0.75	1.11
34		Cu	0.05	0.24	0.28	0.50 (0.16)	0.55	0.78 (0.37)
		Ag	0.17	0.36 (0.26)	0.38	0.58 (0.32)	0.64	0.84 (0.45)
		Au	0.32	0.59	0.60	0.84	1.02	1.20
		Ni	0.12	0.39 (0.16)	0.42	0.72 (0.29)	0.75	1.07 (0.54)
		Pd	0.20	0.48 (0.24)	0.53	0.83 (0.40)	0.94	1.24 (0.66)
35		Cu	0.08	0.26 (0.08)	0.33	0.49	0.62	0.81 (0.47)
		Ag	0.18	0.36 (0.26)	0.39	0.59 (0.35)	0.65	0.84 (0.56)
		Au	0.29	0.54 (0.28)	0.57	0.81 (0.54)	0.95	1.13 (0.85)
		Ni	0.15	0.41 (0.21)	0.47	0.74 (0.37)	0.82	1.09 (0.67)
		Pd	0.23	0.50 (0.27)	0.56	0.86 (0.48)	0.97	1.28 (0.82)
48		Cu	0.05	0.25	0.28	0.51	0.54	0.78 (0.65)
		Ag	0.16	0.35	0.33	0.54	0.50	0.72
		Au	0.27	0.52	0.53	0.81	0.77	1.00
		Ni	0.13	0.35 (0.33)	0.38	0.68 (0.57)	0.68	0.99
		Pd	0.17	0.49	0.48	0.83	0.77	1.33
49		Cu	0.08	0.29	0.33	0.56	0.61	0.83
		Ag	0.17	0.35	0.34	0.54	0.51	0.73
		Au	0.26	0.54	0.53	0.88	0.82	0.99
		Ni	0.16	0.42	0.44	0.73	0.74	1.04
		Pd	0.19	0.50	0.51	0.85	0.79	1.15
50		Cu	0.08	0.26 (0.08)	0.34	0.51 (0.22)	0.62	0.81 (0.47)
		Ag	0.18	0.36 (0.26)	0.38	0.58 (0.34)	0.65	0.84 (0.56)
		Au	0.29	0.54 (0.28)	0.52	0.83 (0.57)	0.95	1.13 (0.85)
		Ni	0.15	0.41 (0.21)	0.47	0.73 (0.36)	0.82	1.09 (0.67)
		Pd	0.23	0.50 (0.27)	0.55	0.86 (0.47)	0.97	1.28 (0.82)
51		Cu	0.13	0.28 (0.12)	0.40	0.53 (0.36)	0.70	0.90 (0.69)
		Ag	0.19	0.36 (0.28)	0.40	0.58 (0.48)	0.67	0.85 (0.72)
		Au	0.30	0.55 (0.44)	0.53	0.83 (0.69)	0.91	1.20 (0.99)
		Ni	0.21	0.43 (0.26)	0.53	0.76 (0.55)	0.89	1.12 (0.86)
		Pd	0.26	0.53 (0.34)	0.60	0.89 (0.66)	1.02	1.32 (1.04)

(NNN) bond energy is easier since one can construct a sufficiently large set of configurations that include only NNN bonds with no NN bonds. In the case of NN bonds, most of the relevant configurations also include NNN bonds [Fig. 5(a)]. Similarly, considering an atom on top of a bridge site, typical configurations that include atoms adjacent to the bridge site exhibit NN bonds between them as shown in Fig. 5(b).

Therefore, we will first examine the additivity of the NNN bonds employing a series of four configurations in which an adatom has 1, 2, 3, and 4 NNN on the surface. For each one of these four configurations the total energy is compared to that of a configuration with the same number of adatoms, in which they are far apart from each other. In Fig. 6(a), the total binding energy between adatoms is plotted as a function of the number of NNN bonds. The best linear fit is drawn, and its slope yields a value of $E_{\rm NNN}=0.0512\,$eV. The next step is to examine the linearity of the NN binding energy using a series of four configurations in which an adatom has 1, 2, 3, and 4 NN's on the surface, within a similar procedure. The NNN bonds in each configuration are deducted using the value obtained before. The results are shown in Fig. 6(b) and the NN bond energy is obtained: $E_{\rm NN}=0.324\,$eV. A similar analysis for an adatom on a bridge site is shown in Fig. 6(c) and the binding energy between an atom on the bridge site and an adjacent atom is given by $E_{\rm NN(bridge)}=0.345\,$eV.
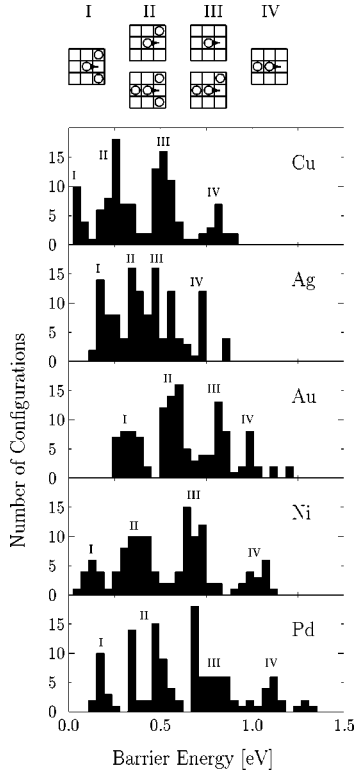
FIG. 3. The distribution of activation energies barriers for Cu(001), Ag(001), Au(001), Ni(001), and Pd(001), obtained from the EAM calculations combined with the molecular statics procedure. The columns represent the number of local configurations, out of the 128 configurations of Fig. 2, giving rise to energy barriers in a certain energy range. Four groups of moves are identified in each of the five plots, and representative moves in each group are shown.
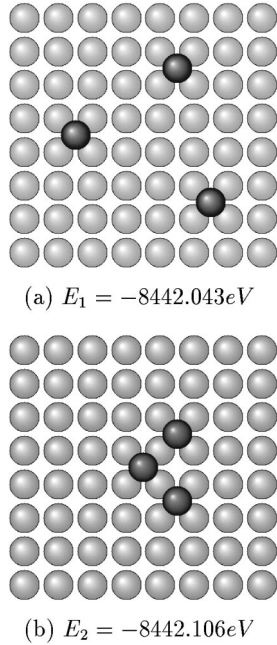

(a) $E_1 = -8442.043 eV$

(b) $E_2 = -8442.106 eV$

FIG. 4. The procedure used to evaluate the binding energies. The binding energy due to two NNN bonds of Cu adatoms on Cu(001) is evaluated as the difference between the total energy $E_1 = -8442.043$ eV of a configuration including three separate adatoms (a) and the total energy $E_2 = -8442.106$ eV of a configuration including three adatoms forming two NNN bonds.
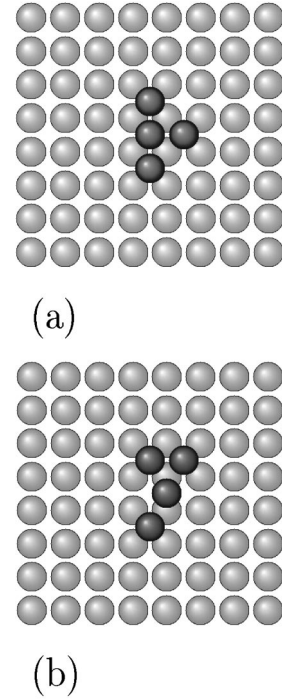

FIG. 5. Configurations used to evaluate the NN bond energy: (a) two nearest neighbors of an adatom may be next nearest neighbors of each other; (b) two nearest neighbors of an atom at the bridge site, may also be nearest neighbors of each other.

B. Construction of the models

The energy barrier E_B for a certain process is the difference between the binding energies of the hopping adatom (to the substrate and to adjacent adatoms) at the initial position, E_{in}, and at the bridge site, E_{top}, namely $E_B = E_{top} - E_{in}$. On the basis of the additivity feature just demonstrated, we will now express these binding energies as the sum of the occupation states of the relevant sites. The first approximation for the energies gives a model (model I) with only two parameters, that reproduces the main features of the EAM barriers. In order to establish the model, there are two things to note about the parameters obtained in Sec. IV A. First, the values of NN binding energies at the lattice site and bridge site are very close. This reflects the fact that the NN distance corresponds approximately to the minimum potential of the two-body interaction. Second, both these energies are much larger than the NNN binding energy. These two features are quite general and common to all the metals we discuss here. For the simplest model we will neglect the effect of the NNN atoms, and assume a single NN binding energy ΔE_{NN} for both lattice and bridge sites. The resulting expression for the binding energy at the initial (fourfold hollow) site is

$$E_{in}^n = E_{in}^0 - \Delta E_{NN}(S_1 + S_3 + S_5). \qquad (4)$$

The energy of an isolated atom is E_{in}^0. The energy of the hopping atom when it is on the bridge site is given by

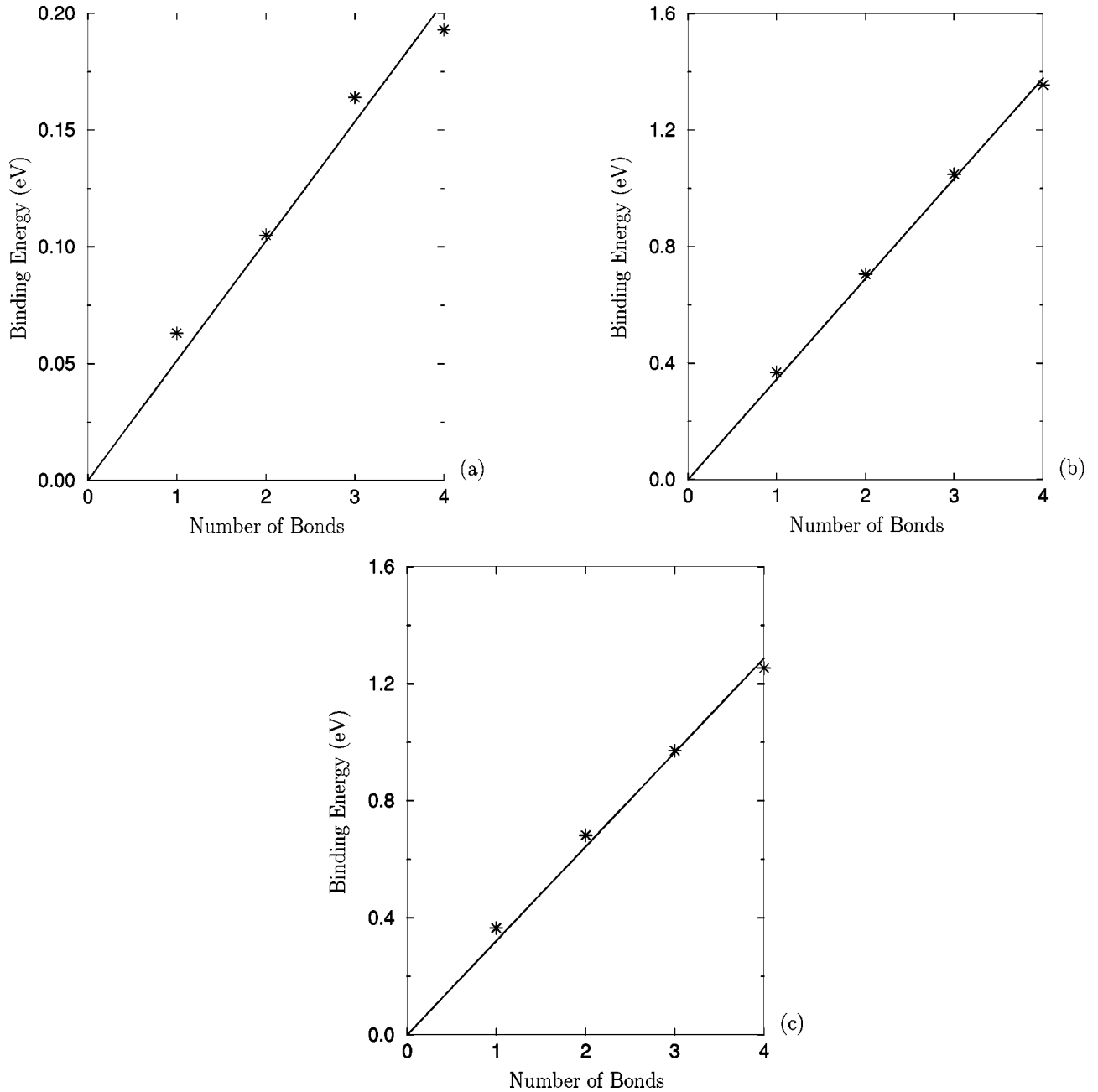$$E_{top}^n = E_{top}^0 - \Delta E_{NN}(S_1 + S_2 + S_5 + S_6), \qquad (5)$$

FIG. 6. Testing the additivity assumption for bond energies on the Cu(001) surface. (a) Binding energy vs the number of NNN bonds. The best linear fit yields a value of $E_{NNN} = 0.0512$ eV; (b) binding energy vs number of NN bonds, where the binding energy of NNN bonds is subtracted. The slope of the solid line yields $E_{NN} = 0.324$ eV; (c) binding energy vs number of NN bonds for an atom at the bridge site, where other NN bond energies are subtracted. The best fit is $E_{top} = 0.345$ eV. The fits include a constraint that the line passes through the origin, since an isolated adatom has zero adatom-adatom binding energy.

where E_{top}^0 is the energy of an isolated atom on top of a bridge site. Thus, for a given configuration the barrier, $E_B^n = E_{top}^n - E_{in}^n$, for an atom to hop into an adjacent vacant site is given in model I by

$$E_B^n = E_B^0 + \Delta E_{NN}(S_3 - S_2 - S_6), \qquad (6)$$

where $E_B^0 = E_{top}^0 - E_{in}^0$ and n is given by Eq. (2). In this model only three sites affect the energy barrier, which can take only four different values, as the expression in the parenthesis can be either 1, 0, -1, or -2. Each of these four barrier values corresponds to one of the four groups in Fig. 3. The param-

eters of this model, as well as those of the models discussed below, are adjusted to best fit the EAM data. More specificly, we found the parameters that best describe the 128 EAM barriers by minimizing the sum of squares

$$R = \sum_{n=0}^{127} [E_B^n(EAM) - E_B^n(Model)]^2. \qquad (7)$$

The values obtained for these parameters for the five metals are shown in Table II. Despite its simplicity, model I can be used to describe and analyze the main diffusion processes: single adatom hopping, attachment, detachment and edge

TABLE II. The parameters E_0, ΔE_{NN}, and ΔE_{NNN} of model II obtained from the best fit of the EAM barriers for Cu, Ag, Au, Ni, and Pd. The values in parenthesis are the corresponding values for model I. R is the sum of squares defined in Eq. (7), for the optimized parameters.

Metal	Model parameters [eV]			R
	E_0	ΔE_{NN}	ΔE_{NNN}	
Cu	0.487 (0.534)	0.274 (0.255)	0.027	0.280 (0.345)
Ag	0.509 (0.525)	0.204 (0.197)	0.010	0.450 (0.458)
Au	0.776 (0.752)	0.235 (0.244)	−0.014	1.275 (1.292)
Ni	0.645 (0.697)	0.326 (0.306)	0.031	0.444 (0.526)
Pd	0.760 (0.789)	0.337 (0.325)	0.017	0.866 (0.892)

TABLE III. The parameters E_0, ΔE_{NN}, ΔE_{NNN}, and ΔE_{opp} of model III obtained from the best fit of the EAM barriers for Cu, Ag, Au, Ni, and Pd. R is the sum of squares defined in Eq. (7).

Metal	Model parameters [eV]				R
	E_0	ΔE_{NN}	ΔE_{NNN}	ΔE_{opp}	
Cu	0.474	0.258	0.044	0.011	0.159
Ag	0.461	0.225	0.013	0.112	0.085
Au	0.686	0.294	−0.017	0.199	0.346
Ni	0.610	0.322	0.046	0.067	0.141
Pd	0.690	0.362	0.028	0.146	0.162

diffusion. The barriers obtained from this model can be incorporated in simulations to reproduce (at least qualitatively) experimental features such us cluster mobility, island morphology and island density.[59]

The model presented above describes only the gross features of the diffusion process. In order to get more quantitative results, and to better understand the importance of the different processes, it is necessary to further refine the model. We will now introduce model II, in which the effect of NNN atoms in the initial configuration is included. The expression for the energy at the initial site is now

$$E_{in}^n = E_{in}^0 - \Delta E_{NN}(S_1 + S_3 + S_5) - \Delta E_{NNN}(S_0 + S_2 + S_4 + S_6), \tag{8}$$

where ΔE_{NNN} is the reduction of the energy due to a NNN bond. The energy barriers are now given by

$$E_B^n = E_B^0 + \Delta E_{NN}(S_3 - S_2 - S_6) + \Delta E_{NNN}(S_0 + S_2 + S_4 + S_6). \tag{9}$$

Model II accounts better for processes such as detachment, edge diffusion, and vacancy diffusion, which generally involve NNN interactions. In the distribution of the barriers obtained from the model, the main groups exhibit certain widths. Yet, they are still significantly narrower than the groups of the EAM barriers. This is due to the fact that during the hopping process adjacent atoms may relax within their potential well. Model II accounts for these effects only on average and therefore gives rise to narrower groups. The values obtained as best fits of the model parameters to the EAM data for the different metals are shown in Table II. Further refinement can be obtained by introducing a distinction between the NN bond energies at the initial four-fold hollow site and that at the bridge site, as suggested in Ref. 59. This modification, which introduces a fourth parameter into the model, gives only slightly better agreement with the EAM results. In the following section, we present a more effective refinement based on nonlinear interactions.

C. Adding nonlinear effects

To obtain models that provide a better fit to the EAM barriers, it is necessary to consider effects that are caused by the simultaneous interactions of the hopping atom with several of its neighbors. Such effects may be described by expressions such us $S_i S_j$ or $S_i S_j S_k$, which are equal to 1 only if all the relevant sites are occupied, and 0 otherwise. Such expressions are clearly beyond the linear bond counting scheme of the previous section. There is a large number of possible nonlinear interaction terms. Our analysis of the EAM calculations, however, indicates that two of them are most significant. The first term is related to the shape of the diffusion path. It corresponds to configurations in which sites adjacent to the bridge site, are occupied on both sides of the diffusion path (namely, at least one of the sites 1 and 2, as well as at least one of the sites 5 and 6 are occupied). It appears that in these cases the energy barrier is considerably higher than for configurations where sites on only one side of the path are occupied. This effect is due to the ''stiffness'' of the diffusion path induced by the attraction from two opposite directions. Even though there are nine different such configurations, they all contribute about the same energy difference, and hence, can be bound to a single parameter ΔE_{opp} (for opposite). The additional term that is now added to the expression for the barrier is ΔE_{opp} $(S_{1,2}S_{5,6})$ where $S_{i,j} = 1$ if at least one of the sites i and j is occupied, and 0 if both are empty. In all the metals we checked, except Cu, this term is much larger than the NNN bond, sometimes by an order of magnitude.

The second nonlinear interaction term is smaller, and is comparable to the effect of NNN sites. It is related to the energy of the hopping atom in the initial site. The EAM calculations indicate that if the two nearest-neighbor sites 1 and 5, that are symmetric with respect to the hopping direction are both occupied, then the initial configuration is more tightly bound. This means that if sites 1 and 5 are both occupied, the energy barrier is expected to be higher. Consequently, the corresponding term would be ΔE_{symm} $(S_1 S_5)$. The fitted value obtained for ΔE_{symm} is very close to that obtained for the NNN binding energy E_{NNN}, for all five metals. We thus included both contributions in the same term, although of different physical origin, to avoid the need for a fifth independent parameter.

The resulting model (model III) for the hopping energy barriers is

$$E_B^n = E_B^0 + \Delta E_{NN}(S_3 - S_2 - S_6) + \Delta E_{opp}(S_{1,2}S_{5,6})$$
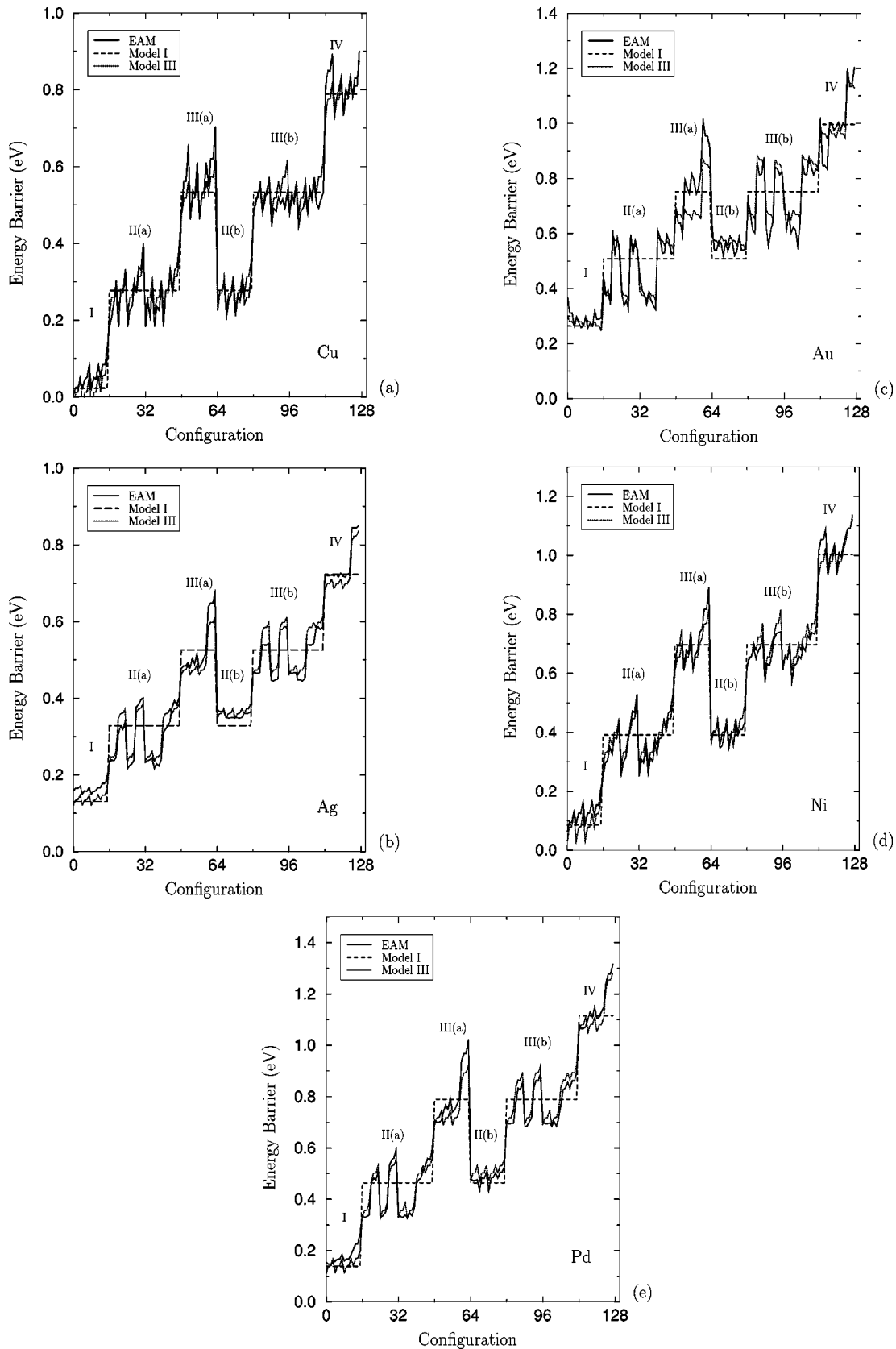$$+ \Delta E_{NNN}(S_0 + S_4 + S_1 S_5). \tag{10}$$

FIG. 7. The hopping energy barriers for (a) Cu, (b) Ag, (c) Au, (d) Ni, and (e) Pd, as a function of the configuration number, which is given by the decimal representation of the binary number $n' = S_3 \bar{S}_2 \bar{S}_6 S_1 S_5 S_0 S_4$. The solid lines are the EAM energy barriers, the dashed lines describe the best fits obtained for model I and the dotted lines are the best fits for model III. Model III is found to provide good quantitative agreement with the EAM results for most configurations. There are essentially 6 groups of barriers in each plot, which correspond to the six columns of Table I. Groups II(a) and II(b) are in the same energy range, and together form group II in Fig. 3, while groups III(a) and III(b) coincide with group III in Fig. 3.

The values obtained from the best fit for the four parameters E_B^0, ΔE_{NN}, ΔE_{opp}, and ΔE_{NNN} for the different metals are given in Table III. There are two remarks to be made about Eq. (10). First, terms such as $S_1 S_5$ are *not* in contradiction to the assumption that only nearest- and next-nearest-neighbor interactions are significant. These terms are just a manifestation of the simultaneous interactions of, say the atoms in sites S_1 and S_5, with the hopping atom, of which they are both nearest neighbors. Second, S_2 and S_6 are not included in the last term of Eq. (10), since we found that their dominant contribution is in the nonlinear term.

D. Testing the quality of the fit

The quality of the fit can be viewed in Fig. 7. The numbering of the configurations is the decimal representation of the binary number $n' = S_3 \bar{S}_2 \bar{S}_6 S_1 S_5 S_0 S_4$, where $S_i = 1(0)$ if site i is occupied (unoccupied), and $\bar{S}_i$ is the opposite of S_i. There are essentially 6 groups of barriers that are marked in the figures. These groups correspond (not necessarily in order) to the six columns of Table I. As can be seen, groups II(a) and II(b) are in the same energy range, and together form group II in Fig. 3. Similarly, groups III(a) and III(b) coincide with group III in Fig. 3. Thus, there are actually only four groups as mentioned in Sec. III. Beyond this basic division, there are some significant differences among the metals which model III seems to handle well. The most important one is the effect of NNN atoms on the energy barrier. It can be seen from Table III that for Ag and Pd this effect is almost negligible, while for Cu and Ni it has much greater importance. The effective NNN binding energy for Au is even negative. Although it may be possible to construct models with the same number of parameters that would give better agreement with EAM results for each specific metal alone, our approach is to find the general characteristics of diffusion mechanisms, common to different substrates. The agreement between the EAM barriers and model III is slightly worse for Au than for the other metals. This may be due to substrate relaxation effects, which are found to be more important in this metal, and are not accounted for in the model.

V. DISCUSSION AND SUMMARY

The models presented in the previous section help to identify the main physical mechanisms that determine the activation energies of self-diffusion processes on fcc (001) metal surfaces. Although such processes may involve interactions with many substrate and in-plane atoms, they can be well described as the sum of few relatively simple terms. The first term is the activation energy for hopping of an isolated atom. The main corrections are due to nearest-neighbor in-plane atoms at the initial site, as well as at the bridge site. The former increase the energy barrier while the latter decrease it by nearly the same amount. The next contribution is due to simultaneous presence of atoms on both sides of the hopping

atom relative to the hopping path. This term is important in relatively dense environments. Its typical value is about half that of the NN binding energy. A third and generally much smaller contribution consists of NNN bonds as well as a term associated with the simultaneous presence of atoms in both sites 1 and 5 (Fig. 2).

Beyond the physical understanding gained by this analysis, the models can be used to evaluate the activation energy of any diffusion process on the (001) surface of the metals discussed above. The models suggest that given a set of few activation energies (which can be obtained from EAM, *ab initio* calculations or experiments), it is possible to extract the complete set of activation energy barriers. To realize model I, for example, only two parameters are needed. They can be obtained, e.g., from the activation energy for single-adatom hopping, and the dissociation energy of a dimer. To estimate a barrier using model II, a third parameter is needed, which is the NNN binding energy. This may be obtained if the mobility of a trimer is known. The fourth parameter, which is needed for model III, can be estimated from the activation energy for detachment from an atomic step. Since model III provides an expression for the energy barriers, linear in the parameters, any four barriers that give rise to four linearly independent equations, are sufficient to determine all four parameters, and consequently all the other barriers.

The possibility to construct a full set of activation energy barriers from a relatively small set of parameters is especially useful for simulations. Without this knowledge, some processes have to be discarded from the simulations as unimportant, or assigned activation energies that are not fully substantiated. These approaches take much of the power of computer simulations, and deny the possibility of direct quantitative confrontation with experimental data. Even if a list of all relevant activation energies is available, the model can be used to check the self consistency of the data. It can also help to interpret simulation results, which depend otherwise on a large number of parameters.

The models presented here apply for diffusion on flat surfaces and do not describe the motion up/down steps. Such interterrace moves involve a large number of possible local environments, including flat steps as well as kink sites. We believe that the approach proposed here can be extended to describe these processes as well.

In summary, we have constructed a family of models that describe self-diffusion on fcc (001) metal surfaces and tested them for Cu, Ag, Au, Ni, and Pd. For each one of these metals, the parameters of the models were optimized by comparing the energy barriers to a full set of barriers obtained from semiempirical potentials via the embedded atom method. It is found that these models, with at most four parameters, provide a good description of the hopping energy barriers on the fcc (001) surfaces.

[1] R. Kunkel, B. Poelsema, L. K. Verheij, and G. Comsa, Phys. Rev. Lett. **65**, 733 (1990).

[2] S. Esch, M. Hohage, T. Michely, and G. Comsa, Phys. Rev. Lett. **72**, 518 (1994).

[3] H. J. Ernst, F. Fabre, and J. Lapujoulade, Phys. Rev. B **46**, 1929 (1992).

[4] H. J. Ernst, F. Fabre, and J. Lapujoulade, Surf. Sci. **275**, L682 (1992).

[5] W. Li, G. Vidali, and O. Biham, Phys. Rev. B **48**, 8336 (1993).

[6] H.-J. Ernst, F. Fabre, R. Folkerts, and J. Lapujoulade, Phys. Rev. Lett. **72**, 112 (1994).

[7] J.-K. Zuo and J. F. Wendelken, Phys. Rev. Lett. **66**, 2227 (1991).

[8] J.-K. Zuo, J. F. Wendelken, H. Dürr, and C.-L. Liu, Phys. Rev. Lett. **72**, 3064 (1994).

[9] H. Dürr, J. F. Wendelken, and J.-K. Zuo, Surf. Sci. **328**, L527 (1995).

[10] A. K. Swan, Z.-P. Shi, J. F. Wendelken, and Z. Zhang, Surf. Sci. **391**, L1205 (1997).

[11] M. Breeman and D. O. Boerma, Surf. Sci. **269/270**, 224 (1992).

[12] J. A. Stroscio, D. T. Pierce, and R. A. Dragoset, Phys. Rev. Lett. **70**, 3615 (1993).

[13] R. Q. Hwang, J. Schröder, C. Günther, and R. J. Behm, Phys. Rev. Lett. **67**, 3279 (1991).

[14] Y. W. Mo, J. Kleiner, M. B. Webb, and M. G. Lagally, Phys. Rev. Lett. **66**, 1998 (1991).

[15] G. Pötschke, J. Schröder, C. Günther, R. Q. Hwang, and R. J. Behm, Surf. Sci. **251/252**, 592 (1991).

[16] M. Bott, T. Michely, and G. Comsa, Surf. Sci. **272**, 161 (1992).

[17] E. Kopatzki, S. Günther, W. Nichtl-Pecher, and R. J. Behm, Surf. Sci. **284**, 154 (1993).

[18] T. Michely, M. Hohage, M. Bott, and G. Comsa, Phys. Rev. Lett. **70**, 3943 (1993).

[19] H. Röder, E. Hahn, H. Brune, J.-P. Bucher, and K. Kern, Nature (London) **366**, 141 (1993).

[20] J. C. Girard, Y. Samson, S. Cauthier, S. Rousset, and J. Klein, Surf. Sci. **302**, 73 (1994).

[21] S. Günther, E. Kopatzki, M. C. Bartelt, J. W. Evans, and R. J. Behm, Phys. Rev. Lett. **73**, 553 (1994).

[22] J. A. Stroscio and D. T. Pierce, Phys. Rev. B **49**, 8522 (1994).

[23] J. Vrijmoeth, H. A. van der Vegt, J. A. Meyer, E. Vlieg, and R. J. Behm, Phys. Rev. Lett. **72**, 3843 (1994).

[24] K. Bromann, H. Brune, H. Röder, and K. Kern, Phys. Rev. Lett. **75**, 677 (1995).

[25] H. Röder, K. Bromann, H. Brune, and K. Kern, Phys. Rev. Lett. **74**, 3217 (1995).

[26] T. R. Linderoth, J. J. Mortensen, K. W. Jacobsen, E. Lægsgaard, I. Stensgaard, and F. Besenbacher, Phys. Rev. Lett. **77**, 87 (1996).

[27] J.-M. Wen, S.-L. Chang, J. W. Burnett, J. W. Evans, and P. A. Thiel, Phys. Rev. Lett. **73**, 2591 (1994).

[28] J. A. Meyer, P. Schmid, and R. J. Behm, Phys. Rev. Lett. **74**, 3864 (1995).

[29] K. Morgenstern, G. Rosenfeld, B. Poelsema, and G. Comsa, Phys. Rev. Lett. **74**, 2058 (1995).

[30] K. Morgenstern, G. Rosenfeld, and G. Comsa, Phys. Rev. Lett. **76**, 2113 (1996).

[31] W. W. Pai, A. K. Swan, Z. Zhang, and J. F. Wendelken, Phys. Rev. Lett. **79**, 3210 (1997).

[32] C. Chen and T. T. Tsong, Phys. Rev. Lett. **64**, 3147 (1990).

[33] G. L. Kellogg and P. J. Feibelman, Phys. Rev. Lett. **64**, 3143 (1990).

[34] G. L. Kellogg and A. F. Voter, Phys. Rev. Lett. **67**, 622 (1991).

[35] S. C. Wang and G. Ehrlich, Phys. Rev. Lett. **70**, 41 (1993).

[36] G. L. Kellogg, Phys. Rev. Lett. **73**, 1833 (1994).

[37] M. C. Bartelt and J. W. Evans, Phys. Rev. B **46**, 12 657 (1992).

[38] M. C. Bartelt and J. W. Evans, Surf. Sci. **298**, 421 (1993).

[39] Z. Zhang and H. Metiu, Surf. Sci. Lett. **292**, L781 (1993).

[40] J. G. Amar and F. Family, in *Mechanisms of Thin Film Evolution*, edited by S. M. Yalisove, C. V. Thompson, and D. J. Eaglesham, MRS Symposia Proceedings No. 317 (Materials Research Society, Pittsburgh, PA, 1994), p. 167.

[41] G. S. Bales and D. C. Chrzan, Phys. Rev. B **50**, 6057 (1994).

[42] G. T. Barkema, O. Biham, M. Breeman, D. O. Boerma, and G. Vidali, Surf. Sci. Lett. **306**, L569 (1994).

[43] M. Breeman, G. T. Barkema, and D. O. Boerma, Surf. Sci. **303**, 25 (1994).

[44] P. Jensen, A.-L. Barabási, H. Larralde, S. Havlin, and H. E. Stanley, Phys. Rev. B **50**, 15 316 (1994).

[45] C. Ratsch, A. Zangwill, P. Smilauer, and D. D. Vvedensky, Phys. Rev. Lett. **72**, 3194 (1994).

[46] D. E. Wolf, in *Scale Invariance, Interfaces and Non-Equilibrium Dynamics*, Vol. 344 of *NATO Advanced Study Institute, Series B: Physics*, edited by M. Droz, A. J. McKane, J. Vannimenus, and D. E. Wolf (Plenum, New York, 1994).

[47] Z. Zhang, X. Chen, and M. G. Lagally, Phys. Rev. Lett. **73**, 1829 (1994).

[48] M. Schroeder and D. E. Wolf, Phys. Rev. Lett. **74**, 2062 (1995).

[49] J. G. Amar and F. Family, Phys. Rev. Lett. **74**, 2066 (1995).

[50] C. Ratsch, P. Smilauer, A. Zangwill, and D. D. Vvedensky, Surf. Sci. Lett. **329**, L599 (1995).

[51] G. S. Bales and D. C. Chrzan, Phys. Rev. Lett. **74**, 4879 (1995).

[52] J. G. Amar and F. Family, Thin Solid Films **272**, 208 (1996).

[53] M. Breeman, G. T. Barkema, M. H. Langelaar, and D. O. Boerma, Thin Solid Films **272**, 195 (1996).

[54] I. Furman and O. Biham, Phys. Rev. B **55**, 7917 (1997).

[55] A. F. Voter, Phys. Rev. B **34**, 6819 (1986).

[56] S. Clarke and D. D. Vvedensky, J. Appl. Phys. **63**, 2272 (1988).

[57] J. Jacobsen, K. W. Jacobsen, P. Stoltze, and J. K. Norskov, Phys. Rev. Lett. **75**, 2295 (1995).

[58] M. Biehl, W. Kinzel, and S. Schinzer, Europhys. Lett. **41**, 443 (1998).

[59] O. Biham, I. Furman, M. Karimi, G. Vidali, R. Kennett, and H. Zeng, Surf. Sci. **400**, 29 (1998).

[60] L. Hansen, P. Stoltze, K. W. Jacobsen, and J. K. Norskov, Phys. Rev. B **44**, 6523 (1991).

[61] L. Hansen, P. Stoltze, K. W. Jacobsen, and J. K. Norskov, Surf. Sci. **289**, 68 (1993).

[62] L. S. Perkins and A. E. DePristo, Surf. Sci. **294**, 67 (1993).

[63] C. L. Liu, J. M. Cohen, J. B. Adams, and A. F. Voter, Surf. Sci. **253**, 334 (1991).

[64] G. Boisvert and L. J. Lewis, Phys. Rev. B **56**, 7643 (1997).

[65] M. Karimi, T. Tomkowski, G. Vidali, and O. Biham, Phys. Rev. B **52**, 5364 (1995).

[66] A. R. Allnat and A. B. Lidiard, *Atomic Transport in Solids* (Cambridge University Press, Cambridge, 1993).

[67] M. S. Daw and M. I. Baskes, Phys. Rev. Lett. **50**, 1285 (1983).

[68] J. B. Adams, S. M. Foiles, and W. G. Wolfer, J. Mater. Res. **4**, 102 (1989).

[69] S. M. Foiles, M. I. Baskes, and M. S. Daw, Phys. Rev. B **33**, 7983 (1986).

[70] M. W. Finnis and J. E. Sinclair, Philos. Mag. A **50**, 45 (1984).